Poly(styrene-*graft*-ethylene oxide) as a Compatibilizer in Polystyrene/Polyamide Blends

PATRIC JANNASCH and BENGT WESSLÉN*

Lund Institute of Technology, Chemical Center, Department of Chemical Engineering II, P.O. Box 124, S-221 00 Lund, Sweden

SYNOPSIS

Polystyrene (PS) blends containing a dispersed phase of either polyamide-6 (PA-6) or polyamide-12 (PA-12) were compatibilized by additions of 1, 3, or 5 wt % poly(styrene-*graft*-ethylene oxide). The graft copolymers were found to have a stabilizing effect on the domain sizes. Weight average radii of PA-6 domains in compression molded samples were reduced by a factor of 5 with 3 wt % graft copolymer added. The corresponding size reduction for PA-12 domains was by a factor of 3. Also, the domain sizes were more uniformly distributed in blends containing the graft copolymers. Thermal analysis of the blends revealed that compatibilization retarded the PA crystallization, with some PA crystallizing at the PS glass transition. This retarded crystallization is explained as a result of the domain size reduction and by the presence of graft copolymer at the interface. The graft copolymers had a toughening effect on the blends and the impact strength of a PS/PA-12 blend was improved by 65% by adding 3 wt % of graft copolymer. Binary blends of the PA and poly(ethylene oxide) (PEO) were investigated in a separate study to verify miscibility of the graft copolymer side chains and the PA. Hydrogen bonding between PA-6 and PEO was confirmed by IR spectroscopy and partial miscibility was indicated by melting point depressions.

INTRODUCTION

The blending of polymers for production of new tailor-made materials at low cost and for recycling mixed polymeric materials has expanded rapidly in recent years. Although there are some binary polymer blends that are known to be miscible, most polymer blends are immiscible and display phase separated structures. Phase separated polymer systems are often desirable because important properties of the different phases will be retained. However, the prospects of obtaining a practically useful material depend strongly on the proper interfacial tension to control the degree of phase separation, and on the interfacial adhesion to transfer mechanical stresses between the phases.[1] The most attractive method of obtaining useful immiscible polymer blends is by the use of compatibilizers. Compatibilizers, usually block or graft copolymers, are amphiphilic in nature and enrich at interfaces. The presence of the compatibilizer at the interface reduces the interfacial tension, which results in smaller domains, and increases the interfacial adhesion.[1,2]

Blends of polystyrene (PS) with different polyamides (PAs) represent immiscible systems where compatibilization is needed. Most studies on the compatibilization of PS/PA blends have been carried out with functionalized styrene copolymers capable of reacting with amide groups in the PA phase during melt mixing. The result is an *in situ* formed compatibilizer having PA grafts. Reactive styrene copolymers with maleic anhydride,[3-6] glycidyl methacrylate,[6] and methacrylic acid[7] have been investigated. The main difficulty with this approach is to control the degree of grafting and thereby the structure of the compatibilizer. Improper grafting usually results in poor mechanical properties.[6,7] An alternative way to compatibilize PS/PA blends is to add well-defined, premade compatibilizers. However, this procedure requires

* To whom correspondence should be addressed.

Journal of Applied Polymer Science, Vol. 58, 753-770 (1995)
 CCC 0021-8995/95/040753-18

Table I Data of Graft Copolymers

	$\bar{M}_n$ (Main Chain) (g/mol)	$\bar{M}_n$ (Side Chain) (g/mol)	Average MW Between Grafts (g/mol)	PEO Content (wt %)	T_{melt} (°C)	ΔH_f (J/g)[a]	T_c (°C)	ΔH_c (J/g)[a]
SEO18	80,000	10,900	10,400	51	58	64	38	63
SEO20	80,000	4,300	10,400	29	41	19	−20	12
SEO21	10,000	2,500	2,000	55	42	46	−35	19

[a] Based on the sample weight.

a separate synthesis step, which often is difficult to carry out. A suitable premade compatibilizer would be a PS block or graft copolymer carrying segments miscible, or partly miscible, with PA. Fayt and Teyssié[8] used poly(styrene-*block*-methyl methacrylate) to reduce the domain size in PS/PA-6 blends. A much larger effect on the domain size was noted when similar block copolymers with partly hydrolyzed poly(methyl methacrylate) (PMMA) were used. The PMMA blocks, now containing a few percent methacrylic acid groups, were found to react chemically with the PA-6 phase.

Polymers containing ether groups have been found to show some miscibility with PAs.[9] For example, poly(ethylene oxide) (PEO) and other ether group containing polymers have been found to interact with different amorphous PAs through hydrogen bonding.[9,10] In the present work some well-defined graft copolymers with PS main chains and PEO grafts were used as compatibilizing additives in PS/PA-6 and PS/PA-12 blends. The primary objective was to investigate if the interactions between the PEO grafts and the PAs were significant enough to provide compatibilization. Investigations of the compatibilizing ability of PS–PEO copolymers are scarce. The only example known to us is the use of PEO–PS–PEO triblock copolymers in blends of phenolphthalein poly(ether ether ketone) and poly(2,6-dimethyl-1,4-phenylene oxide).[11]

EXPERIMENTAL

Materials

PS–PEO graft copolymers, designated SEO, were prepared by ethoxylation of amide-containing styrene copolymers. The preparation and characterization of these polymers have been described in detail previously.[12] Styrene copolymers were synthesized by free radical copolymerization of styrene and acrylamide. The copolymers were dissolved in 2-ethoxyethyl ether, and the amide groups were ionized by using potassium *tert*-butoxide. Grafting was achieved by utilizing the amide anions as initiator sites for the polymerization of ethylene oxide in 2-ethoxyethyl ether at 80°C. Three different graft copolymers, all with different chain dimensions, were used in this work. The molecular and thermal data of these polymers are shown in Table I. Thermal characterization by differential scanning calorimetry (DSC) is described below.

The homopolymers used were: general purpose PS, VESTYRON® 1202 (Hüls AG), $\bar{M}_n$ = 190,000 g/mol as determined with gel permeation chromatography (GPC), with melt flow rates (MFR) of 16 (230°C, 5 kg) and 3 (200°C, 5 kg); ULTRAMID® B4 polyamide-6 from BASF with MFR of 13 (230°C, 5 kg); VESTAMID® L2101F polyamide-12 (Hüls AG) with MFR of 6 (200°C, 5 kg); and PEO, $\bar{M}_n$ ~ 10,000 g/mol (Schuchardt). MFRs were measured according to ISO 1133 with a Davenport MFR apparatus.

Probing Partial Miscibility and Interactions in PA/PEO Blends

Blends of PA-6/PEO and PA-12/PEO, together with the homopolymers, were investigated by DSC and IR spectroscopy. PA/PEO blends (50/50 w/w) were prepared by solution casting from dilute (10 wt %) formic acid solutions. The casting was done at 60°C in a circulating air oven. After the solvent had evaporated, the blends were dried at 100°C for 2 h to remove residual formic acid, and were then allowed to cool at ambient temperature. Films of the homopolymers were prepared in the same way. Blends and homopolymers were analyzed by DSC, as described below. Transmission IR spectra of the blends and homopolymers were obtained with a Bruker IFS 66 FTIR instrument equipped with a DTGS detector. Analyses were performed at ambient temperature using thin films. The films were made by solution casting from dilute formic

acid solutions at 60°C onto KBr disks. All spectra had maximum absorptions below 0.5.

Melt Mixing

Blends of PS/PA-6 and PS/PA-12 having 0, 1, 3, and 5 wt % of graft copolymer were prepared in a Brabender mixer using screw-type rollers. The weight ratio of PS to PA was in all cases 80 : 20. All homopolymers were vacuum dried for 48 h at 80°C. The graft copolymers were dried for 1 week at ambient temperature under vacuum. Approximately 50 g of a mixture of the various polymers was fed simultaneously to the mixer head. The mixing proceeded for 10 min with a roller rate of 30 rpm, and the mixing temperatures for the PA-6 and PA-12 blends were 230 and 200°C, respectively. The equilibrium Brabender torque was in all cases 8–10 Nm. After mixing, the blends were collected and cooled at ambient temperature before characterization.

Two PS/PA-12 blends, containing 0 and 3 wt % of graft copolymer SEO20, were made with a Berstorff ZE25 corotating twin-screw extruder having a diameter of 25 mm and a length to diameter ratio of 43. The extruder was operated at 200°C with a rotation rate of 100 rpm, and with a feed rate of approximately 100 g/min. These blends were made in larger amounts to enable impact and tensile testing, and to investigate the influence of the mixing method on the morphology.

Morphological Analysis

All blends were compression molded into approximately 0.7-mm thick bars. The different blends were preheated at the respective mold temperature for 2 min. The PA-6 and PA-12 blends were compression molded for 5 min at 230 and 200°C, respectively. After molding, the bars were cooled to room temperature during approximately 4 min. The bars were then quenched in liquid nitrogen and freeze fractured.

The PS phase was dissolved and separated from the PA domains in order to enable determination of the PA domain sizes and size distributions. Pieces of the compression molded samples were immersed in 4 mL of *o*-xylene for 24 h. The resulting suspensions were centrifuged at 3,000 rpm for 20 min. The transparent top phase, containing PS dissolved in *o*-xylene, was removed and the bottom layer containing the PA domains was redispersed in another 4 mL of pure *o*-xylene. This procedure was repeated twice for all samples. After vigorous stirring, a droplet from each suspension was placed on SEM sample

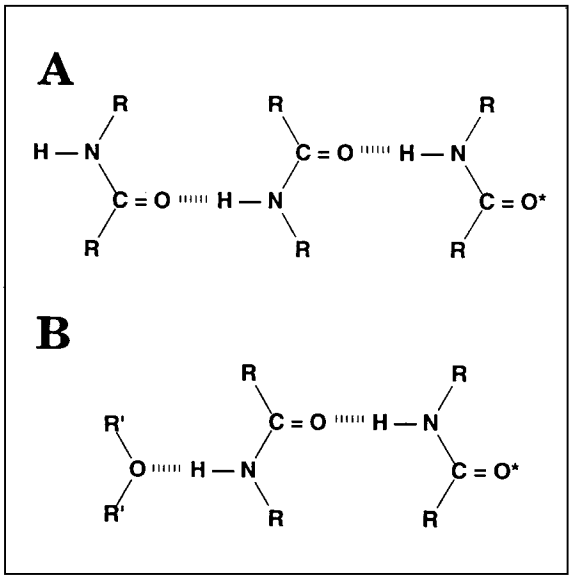

Figure 1 Hydrogen bonding states in (A) a pure PA and (B) a (partly) miscible blend of a PA and a polyether. The fraction of free, nonhydrogen bonded carbonyls (indicated by stars) is larger in the PA/PEO blend, as compared with pure PA.

holders and the *o*-xylene subsequently evaporated at ambient temperature. The solid contents of the transparent top phases collected during the centrifugation procedure were analyzed by IR spectroscopy and were found to contain no PA.

The sample surfaces were coated with 25-*nm* thick layers of Au by sputtering. The samples were examined by scanning electron microscopy (SEM) using an ISI 100A SEM operating at 15 kV. The number-average radius, $\bar{R}_n$, and the weight-average radius, $\bar{R}_w$, of the PA domains in each blend were evaluated from micrographs of isolated PA domains. The radii of at least 1,000 particles were measured for each sample. The average radii are defined as below.

$$\bar{R}_n = \frac{\sum n_i R_i}{\sum n_i} \tag{1}$$

$$\bar{R}_w = \frac{\sum n_i R_i^4}{\sum n_i R_i^3}. \tag{2}$$

The polydispersity index (PDI) is defined as $\bar{R}_w/\bar{R}_n$.

Thermal Characterization

The thermal properties of blends, homopolymers, and graft copolymers were analyzed with a Mettler

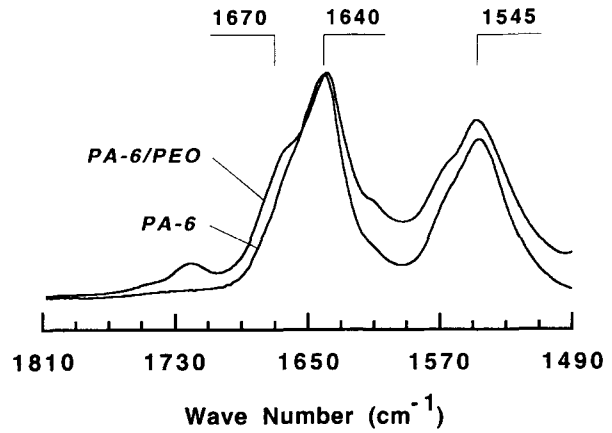

Figure 2 IR spectra in the amide I (at 1640 cm^{-1}) and amide II (at 1545 cm^{-1}) region of pure PA-6 and PA-6/PEO (50/50 w/w). The amide I region contains contributions from hydrogen bonded (at 1640 cm^{-1}) and nonhydrogen bonded carbonyls (at 1670 cm^{-1}). The presence of PEO clearly increases the fraction of nonhydrogen bonded carbonyls, indicating interactions between amide and ether groups.

TA 3000 DSC system. Analyses were made on blend samples of 7–15 mg contained in sealed aluminum pans. PA-6 and blends containing PA-6 were first annealed at 240°C for 5 min. The samples were then cooled down to −100°C, and subsequently reheated to 250°C. PA-12 and PA-12 blends, as well as the pure graft copolymers, were annealed at 190°C for 5 min. After cooling down to −100°C, the samples were reheated to 250°C. The temperature scan rate was in all cases 10°C/min. Homo-PS and homo-PEO were analyzed by both methods and no significant differences in the results were found. The thermograms were evaluated using Mettler Graphware TA72. Glass transition temperatures (T_g) were obtained from the last heating scan and were determined from inflection points. The heats of crystallization (ΔH_c) and of fusion (ΔH_f) were determined by integration of the peak areas and are based on the total sample weights. The temperatures were reported as crystallization (T_c) and melt (T_{melt}) temperatures.

Mechanical Testing

Specimens used for impact and tensile testing were prepared using an Engel ES 200/50HL injection molding machine operating at 200°C. The mold temperature was kept at 50°C. The specimens were vacuum dried for 48 h at 80°C before mechanical testing. Notched and unnotched Charpy impact strength were determined according to ISO/R179 with a CEAST impact tester. The tensile properties were evaluated according to ISO/R527 using a Schenk tensile tester at a crosshead speed of 10 mm/min.

RESULTS AND DISCUSSION

PA-PEO Miscibility and Interactions

Most studies regarding compatibilization of immiscible blends are concerned with compatibilizers containing polymer segments chemically identical to the blend components. A "nonidentical" compatibilizer in which the polymer segments are different from the blend components, but miscible, or at least partly miscible, should be equally efficient in promoting a high degree of phase dispersion and improving interfacial adhesion.[1,2,8,11] In fact, the concept of a nonidentical compatibilizer offers more advantages because a single compatibilizer may be used in several blend systems. This may be especially important when considering recycling of mixed polymeric materials. One of the critical factors determining the success of nonidentical compatibilizers is the miscibility of

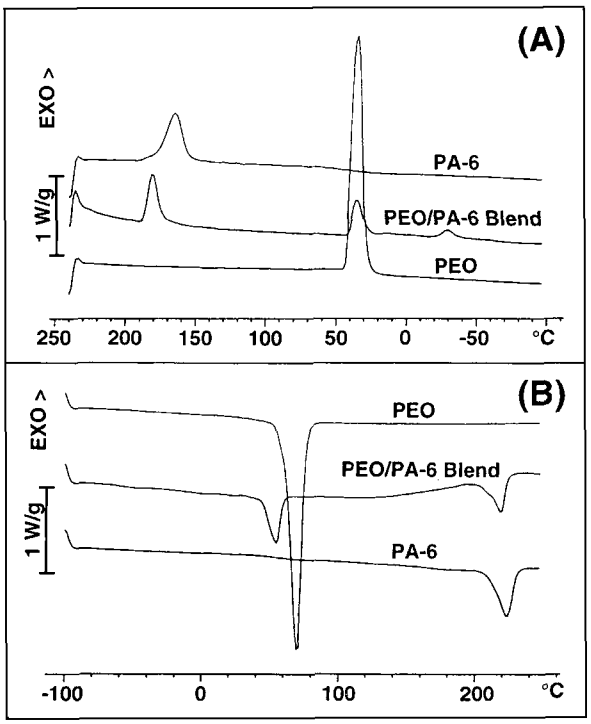

Figure 3 (A) DSC crystallization exotherms for PA-6, PEO, and their binary blend (50/50 w/w). (B) DSC melting endotherms for the same samples. (Values for *W/g* given are based on the total sample weight.)

the different compatibilizer segments with the corresponding blend components.

In the present investigation the compatibilization of PS/PA blends by PS-PEO graft copolymers was studied. The graft copolymers were prepared by ethoxylation of styrene–acrylamide copolymers (see Experimental).[12] Compositions and thermal properties are collected in Table I. The PS main chain of the PS-PEO graft copolymer should be miscible with the PS phase. However, the miscibility of the PEO side chains with the PA phase was not known. A limited study was therefore undertaken to investigate interactions and partial miscibility of PEO with PA-6 and PA-12.

PAs are strongly self-associating because the amide N—H hydrogens act as hydrogen bond donors, and amide C=O groups as hydrogen bond acceptors (see Fig. 1).[9,13] Polyethers, on the other hand, may be regarded as weakly associating polymers.[13] When polyethers are blended with PAs, some amide N—H groups will interact with ether oxygens, which act as hydrogen bond acceptors.[9,10] This interaction will, if significant enough, induce partial miscibility of PEO in PA. Interactions between ether and amide groups will thus leave a larger fraction of "free" (nonhydrogen bonded) C=O groups in the blend than in pure PA.

Hu and coworkers studied hydrogen bonding in different PAs and PA/PEO blends by IR spectroscopy.[10] They found that the amide I mode absorption at approximately 1640 cm^{-1} may be considered to have contributions from C=O stretching, C—N stretching, and C—C—N deformation vibrations. The authors also found that the amide I mode absorption could be resolved into two components: one at 1670 cm^{-1} attributed to free C=O, and one at 1640 cm^{-1} attributed mainly to hydrogen bonded C=O. The amide II mode absorption, having contributions from N—H in-plane bending, C—N stretching, and C—C stretching vibrations, does not display any features that can be assigned to free or hydrogen bonded groups. Figure 2 shows the amide I and II bands in pure PA-6 and in a PA-6/PEO (50/50 w/w) blend. The spectrum of the PA-6/PEO blend clearly shows a substantial contribution from free C=O stretching in the amide I region, which strongly indicates the presence of hydrogen bonding between PEO and PA-6. Spectra from the corresponding PA-12/PEO blend did not show any free C=O stretching band. The concentration of amide groups in PA-12 is roughly half of that in PA-6, which may decrease the number of possible amide–ether interactions considerably.

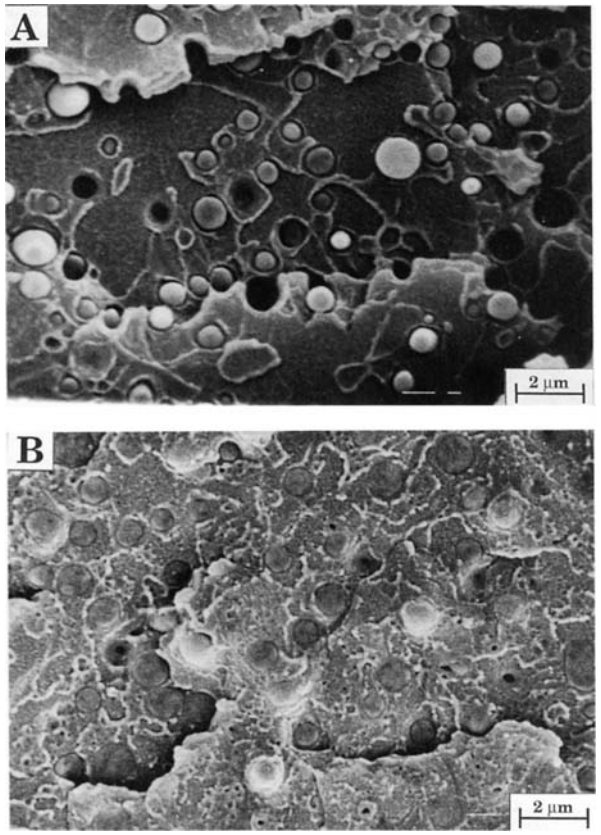

Figure 4 SEM micrographs of freeze-fractured PS/PA-6 blends before compression molding with (A) 0 wt % SEO18 and (B) 5 wt % SEO18.

DSC thermograms showing crystallization exotherms and melting endotherms from PA-6, PEO, and PA-6 blended with 50 wt % PEO are shown in Figure 3. Thermal data for the PA/PEO blends and the homopolymers are collected in Table II. Both PA-6 and PA-12 crystallized at higher temperatures when blended with PEO, indicating that the PEO melt might have a nucleating function. A similar effect has been observed in PA-6 blends with poly(vinylidene fluoride).[14] The PA-6 melting point depression of about 4°C in the presence of PEO is clearly a sign of partial miscibility. This effect was not seen in the PA-12/PEO blend, however. PA-6 and PA-12 influenced the thermal behavior of PEO in a similar way. Crystallization of PEO in the blends was evidently disturbed. At least two separate crystallization processes were observed; one at the normal PEO crystallization temperature and the other at about 15°C lower temperature. Also, the PEO melting point was depressed approximately 10°C in both PA-6 and PA-12 blends.

Table II DSC Results, PA/PEO Blends

Sample	T_{melt} (PA) (°C)	T_{melt} (PEO) (°C)	T_c (PA) (°C)	T_c (PEO) (°C)
PEO	—	64	—	42
PA-6	221	—	168	—
PA-6/PEO	217	54	182	37; −28
PA-12	176	—	139	—
PA-12/PEO	176	56	154	40; −20

From these results it may be concluded that specific interactions, such as hydrogen bonding between PA amide groups and PEO ether oxygens, induce partial miscibility of PEO and the PAs. Not surprisingly, this effect is more significant in the case of PA-6. Because PA-6 contains more amide groups than PA-12 per unit volume, PA-6 can be expected to reach a higher degree of interaction and miscibility with PEO.

Fracture Morphology

Processing of an insufficiently compatibilized immiscible polymer blend may cause a growth in domain size because of shearing and annealing.[1,15] This effect is known as coalescence and is a consequence of the nonequilibrium state of a polymer blend.[1,15] The stabilizing effect of PS–PEO graft copolymers on PS/PA morphologies were studied by evaluating the PA domain sizes of compression molded blends. Blends of PS/PA-6 and PS/PA-12 with 0–5 wt % graft copolymer were prepared in a Brabender mixer at 230 and 200°C, respectively. Two PS/PA-12 blends with 0 and 3 wt % of graft copolymer SEO20 were also prepared by extrusion at 200°C. Figure 4(A,B) shows typical micrographs of freeze-fracture surfaces of compatibilized and uncompatibilized Brabender made blends, respectively, before com-

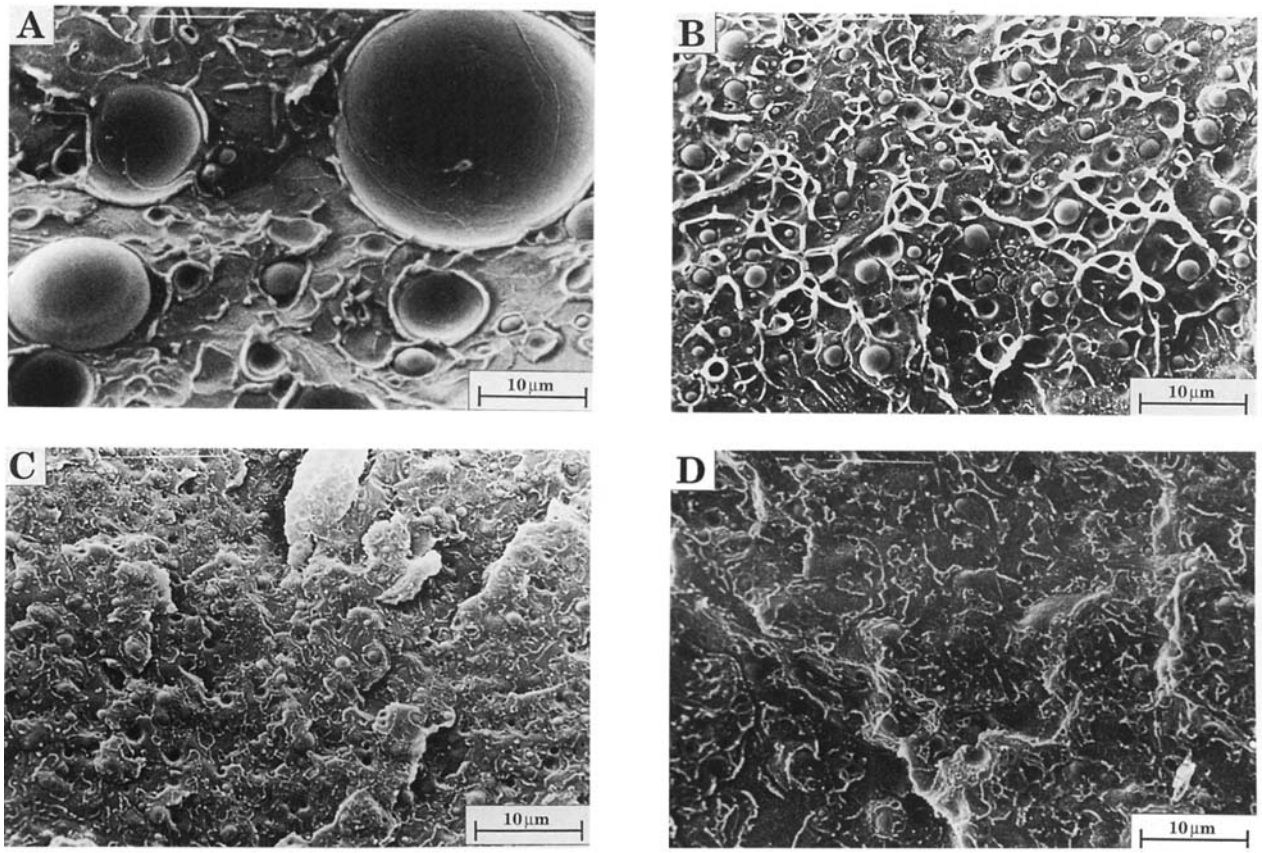

Figure 5 SEM micrographs of freeze-fractured PS/PA-6 blends after compression molding with (A) 0 wt % SEO20, (B) 1 wt % SEO20, (C) 3 wt % SEO20, and (D) 5 wt % SEO20.

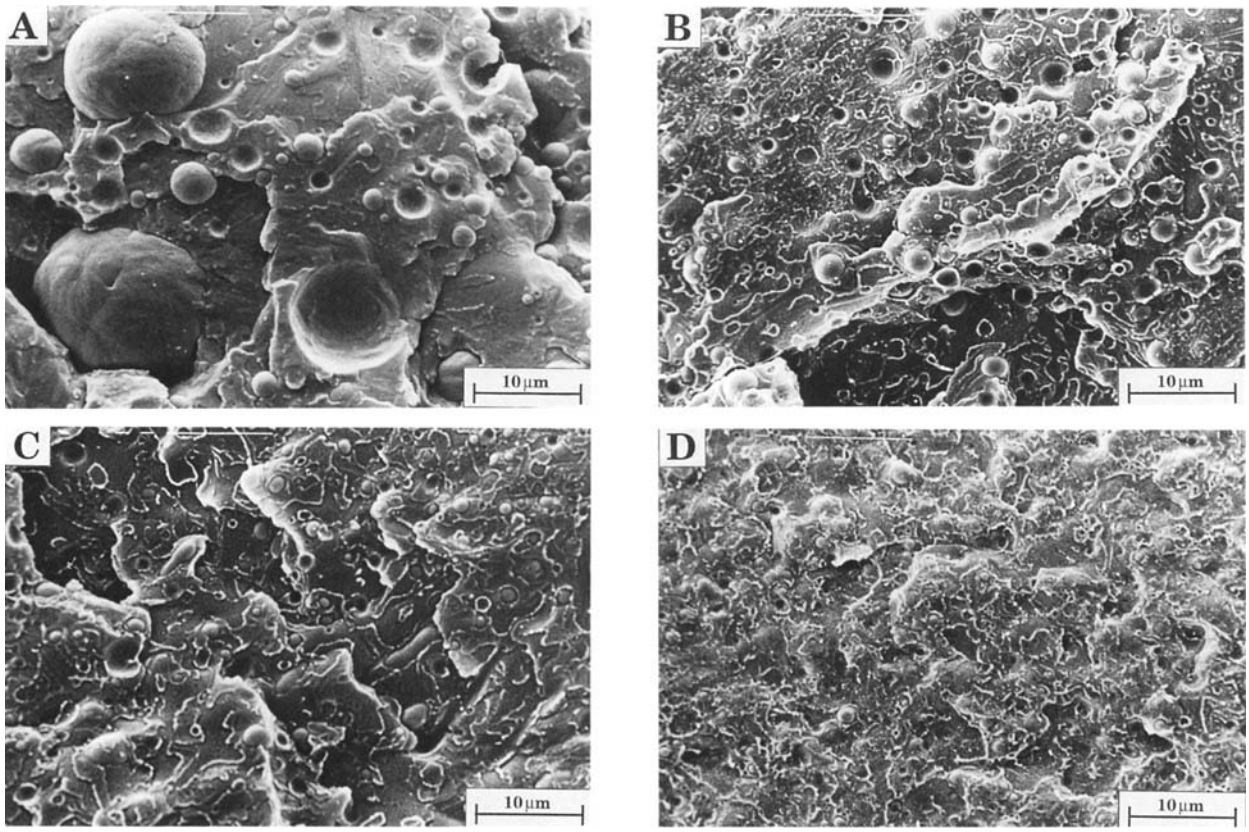

Figure 6 SEM micrographs of freeze-fractured PS/PA-12 blends after compression molding with (A) 0 wt % SEO20, (B) 1 wt % SEO20, (C) 3 wt % SEO20, and (D) 5 wt % SEO20.

pression molding. The graft copolymer seems to have little effect on the domain sizes after melt blending. The PA domains in compatibilized, as well as in the uncompatibilized blends, show a fibrous nature. The surfaces of the compatibilized samples are smoother however, and the PA domains appear to adhere more strongly to the PS matrix. Micrographs of freeze-fractured surfaces after compression molding are shown in Figures 5(A–D) and 6(A–D) for PS/PA-6 and PS/PA-12 blends, respectively. PA domain sizes were now found to depend strongly on the amount of compatibilizer added. The micrographs also clearly show that graft copolymers SEO18 and SEO20 (Table I) were quite efficient in stabilizing the domain sizes in both PA-6 and PA-12 blends. On the other hand, graft copolymer SEO21, which had significantly shorter grafts (Table I), was ineffective as a compatibilizer, and the domain sizes in these blends were seemingly unaffected by additions of the graft copolymer.

PA Domain Size

One of the most common methods to evaluate the domain sizes in an immiscible blend is SEM analysis of an etched flat surface.[3,5,16] Another useful method is transmission electron microscopy (TEM) analysis of stained, microtomed samples.[16] In the present study PA domains were isolated by dissolving the

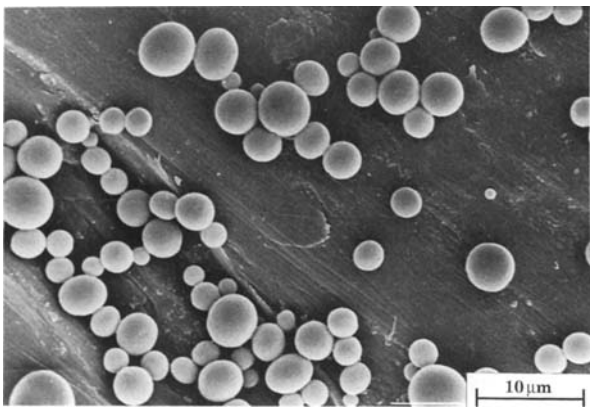

Figure 7 SEM micrograph of free PA-6 domains isolated from the compression molded PS/PA-6 blend with 1 wt % SEO18. After the PS matrix had been dissolved in *o*-xylene, the PA domains were collected by centrifugation for subsequent evaluations of domain sizes and size distributions.

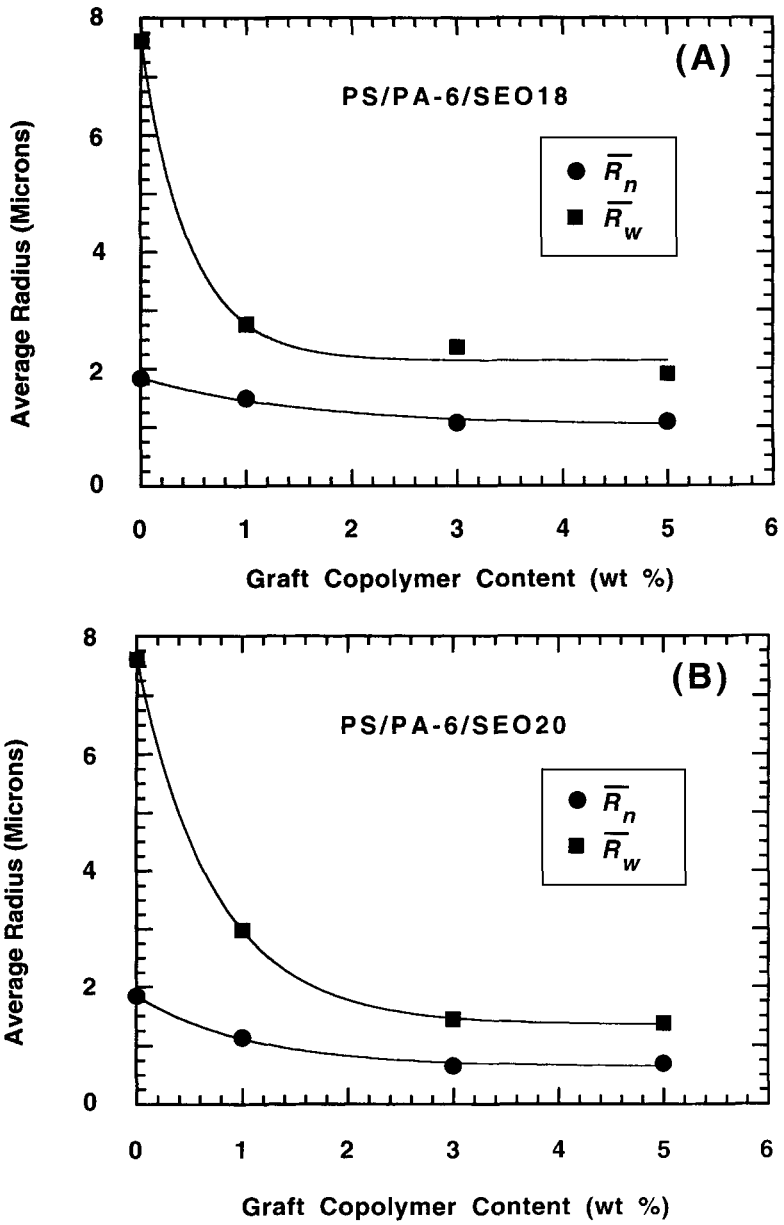

Figure 8 The dependence of the PA domain weight and number-average radii on the PS-PEO graft copolymer content for (A) PS/PA-6 with SEO18, (B) PS/PA-6 with SEO20, (C) PS/PA-12 with SEO18, and (D) PS/PA-12 with SEO20.

PS matrix and subsequent analysis by SEM to evaluate average sizes and size distributions. Advantages offered by this method, in contrast to the above-mentioned ones, are that the equatorial radius can be determined and that a minimum of sample preparation is required. Also, the three-dimensional (3-D) shape of the dispersed phase is more readily observed. One of the disadvantages is that the distribution of domains within the sample cannot be observed. However, this can be compensated for by a parallel SEM study of etched or unetched freeze fractured samples.

Figure 7 shows a typical micrograph of PA domains isolated from a compression molded sample, on a SEM sample holder. Number- and weight-average radii were evaluated from the micrographs, and in Figure 8 they are plotted as functions of the added amount of graft copolymer for the different blends. As mentioned above, blends containing graft copolymer SEO21 were not compatibilized, and

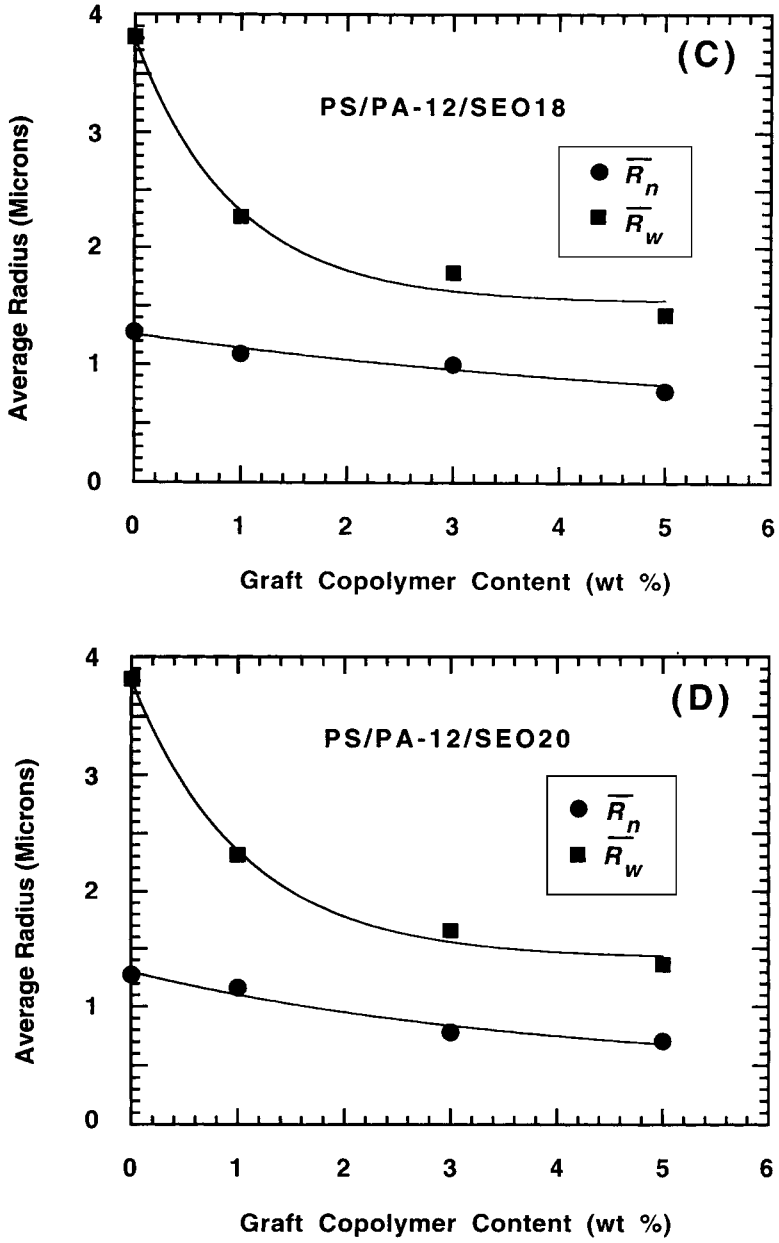

Figure 8 (*Continued from the previous page*)

therefore domain sizes in these blends were not evaluated. The interfaces of all blends seem to be saturated at a concentration of about 3 wt %; no further reduction of the PA domain sizes was noted at larger amounts. The saturation effect and the general features of the curves in Figure 8 have been reported by others[17,18] and can be explained by a theory derived by Taylor[19] on Newtonian dispersed systems in shear flow. Initially, the compatibilizer reduces the interfacial tension, thereby causing a drop in domain size. The final domain size will be determined by a balance of shear forces, causing domain breakup, and interfacial tension, working against deformation and domain breakup. Thus, addition of compatibilizer beyond the saturation concentration will not result in any further decrease in $\bar{R}_n$.

The incompatibility of very short chain segments in a compatibilizer is not high enough to promote a significant interfacial activity.[20] The compatibilizing ability of graft copolymers has been reported to be directly related to the length of the grafts and to the length of the main chain segments between the grafts.[21,22] The low molec-

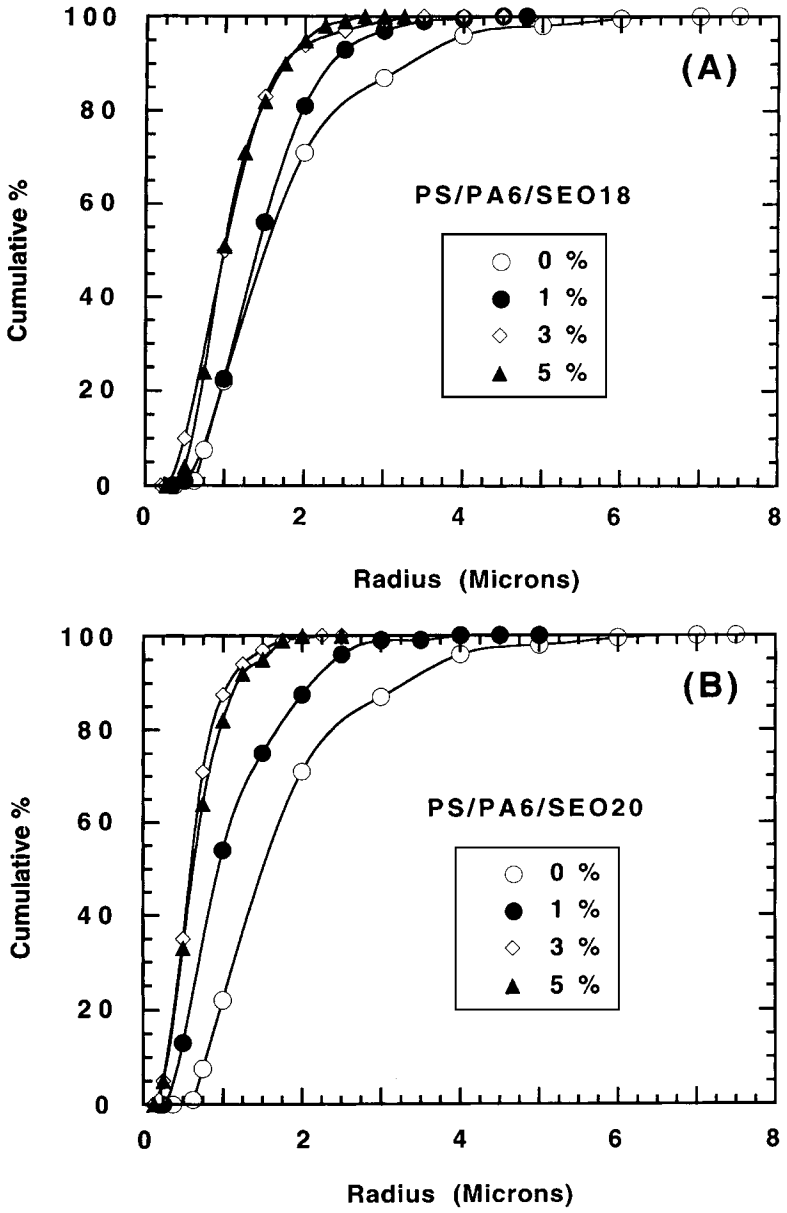

Figure 9 Cumulative (linear) distributions of the PA domain sizes in the blends (A) PS/PA-6 with SEO18, (B) PS/PA-6 with SEO20, (C) PS/PA-12 with SEO18, (D) PS/PA-12 with SEO20 (Brabender mixed), and (E) PS/PA-12 with SEO20 (extruded).

ular weights of the grafts and the chain segments between the grafts of graft copolymer SEO21 (Table I) apparently make it a poor compatibilizer, and it is probably not located at the blend interfaces. Graft copolymers SEO18 and SEO20, on the other hand, have larger segmental and overall molecular weights that should result in higher interfacial coverage. The ability of SEO18 and SEO20 to reduce domain sizes was found to be of the same order for both PA-6 and PA-12 blends. However, it is evident from Figure 8 that the domain size reduction is larger for the PA-6 blends than for the PA-12 blends. Graft copolymer SEO20, for example, reduces the PA-6 weight-average radius by a factor 5.6, while the corresponding reduction for PA-12 is 2.7. Most of this difference is connected to the domain sizes of the uncompatibilized blends, where the PA-6 domains were about twice as large as the PA-12 ones.

Tang and Huang[17] proposed an equation where the average radius, R, of the dispersed phase is given by:

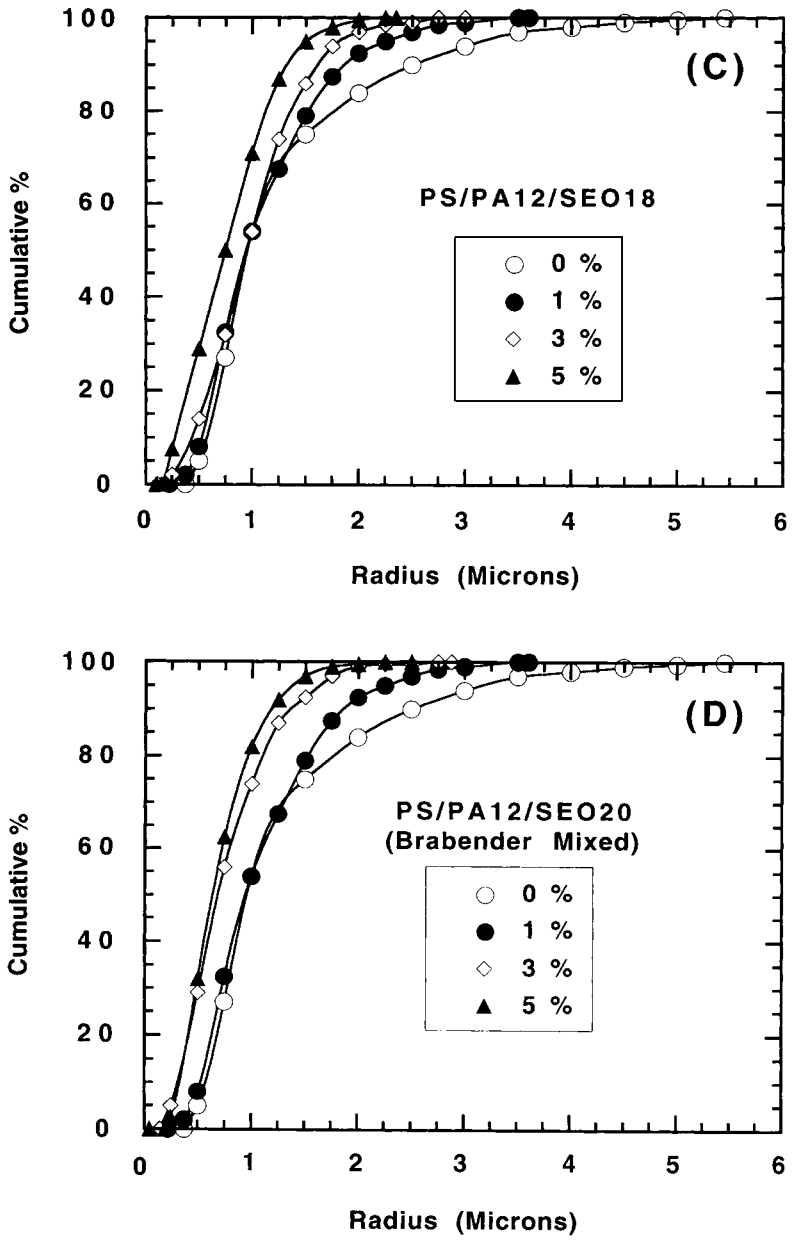

Figure 9 (*Continued from the previous page*)

$$R = (R_0 - R_s)e^{-KC} + R_s \quad (3)$$

where R_0 and R_s are the average radii at compatibilizer concentration zero and at saturation, respectively. The equation is based on the assumption that the change in the interfacial tension with the concentration of compatibilizer is given by:

$$-\frac{d\gamma}{dC} = K(\gamma - \gamma_s) \quad (4)$$

Table III Parameters Fitted to Number-Average Radii

	PS/PA-6 Blends with		PS/PA-12 Blends with	
Parameter	SEO18	SEO20	SEO18	SEO20
K	0.64	0.93	0.20	0.27
R_0	1.9	1.9	1.3	1.3
R_S	1.0	0.7	0.5	0.5

Parameters are defined by eq. (3).

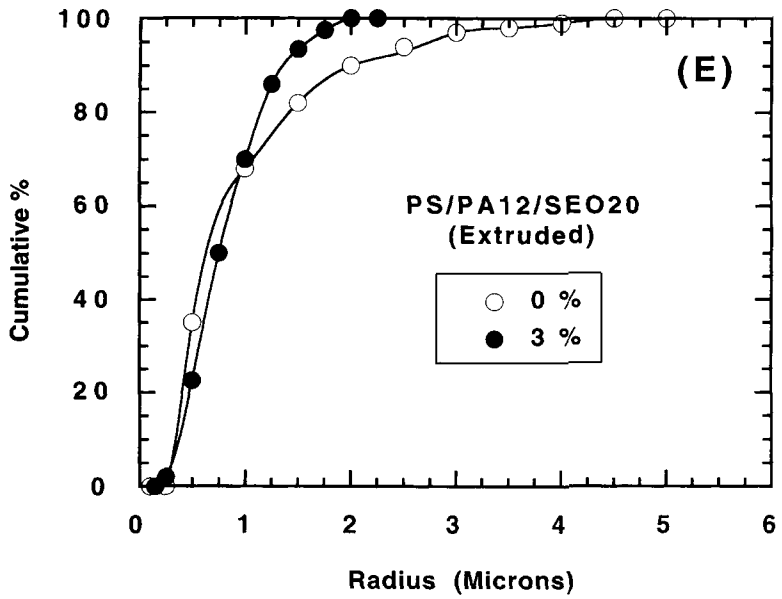

Figure 9 *(Continued from the previous page)*

where γ is the interfacial tension at a compatibilizer concentration C, γ_s is the interfacial tension at the saturation concentration, and K is a constant. The changes of both number- and weight-average radii with compatibilizer concentration were fitted to eq. (3), as shown in Figure 8. The fitted parameters for $\bar{R}_n$ are given in Table III. The constant K can be expected to increase with the segment sizes of the compatibilizer and decrease with the degree of compatibilizer self-association in the blend.[17] The value of K was higher for graft copolymer SEO20, as compared to the value of SEO18, in both PA-6 and PA-12 blends. This implies that SEO20 is a more efficient compatibilizer than SEO18. The PS/PEO ratio of SEO20 may be more suited in the present systems. Graft copolymer SEO20 should have a lower degree of self-association, as a result of its shorter PEO grafts. PA-6 blends compatibilized with SEO20 also displayed a lower R_s value (Table III). No corresponding difference was noted for the PA-12 blends.

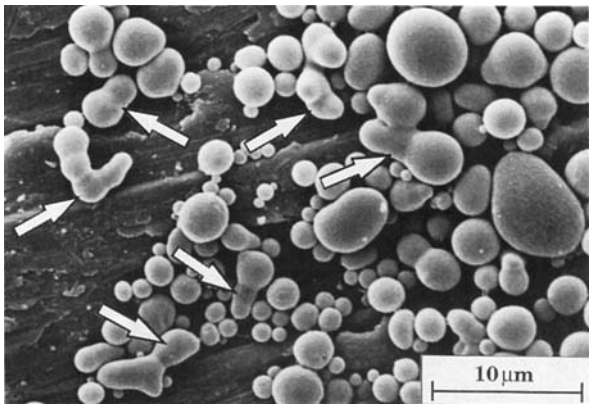

Figure 10 SEM micrograph showing aggregated PA-6 domains (indicated by arrows) from the compression molded PS/PA-6 blend with 5 wt % SEO20. The micrograph shows isolated domains.

PA Domain Size Distribution

Additions of graft copolymers SEO18 and SEO20 not only reduce the PA domain sizes but also narrowed the size distributions. Cumulative distributions of domain sizes determined for the compression molded PA-6 and PA-12 blends are shown in Figure 9(A,B) and 9(C–E), respectively. The uncompatibilized blends contained a significantly higher percentage of large domains, formed through coalescence, than the compatibilized ones. Some domains with radii in the region of 15 μm were found. As the amount of graft copolymer increased, the PDI decreased (Fig. 8), and at 5 wt % of graft copolymer the PDI of the PA-6 blends had decreased by about 60%. The corresponding decrease for the PA-12 blends was about 40%. The cumulative distributions found for the PA-6 blends with 3 and 5% graft copolymer were nearly identical, which indicated a saturation at the 3% level.

PA Domain Aggregation

As mentioned earlier, the final domain size in an immiscible blend depends on a dispersion–coales-

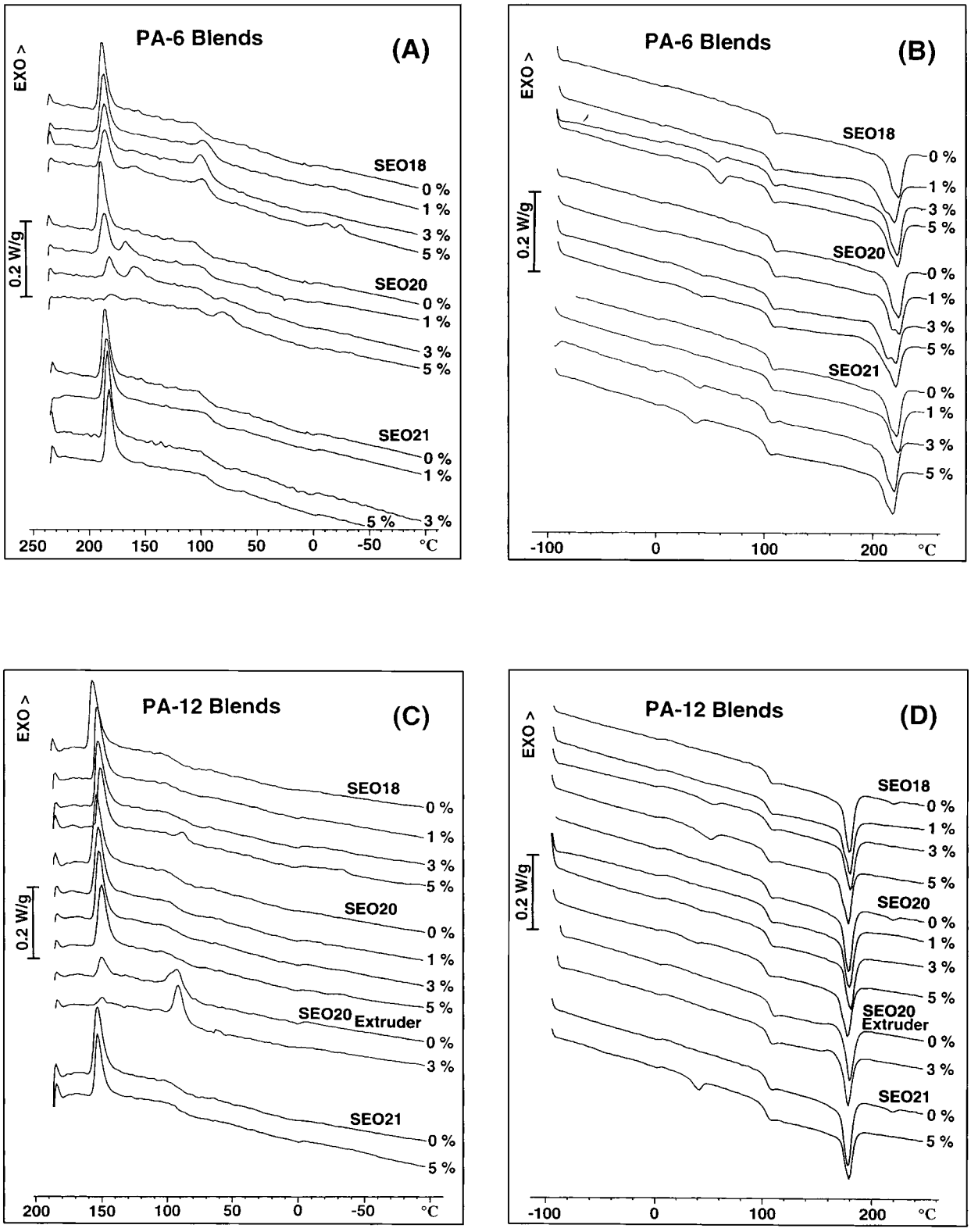

Figure 11 Thermograms of PS/PA-6 and PS/PA-12 blends with various amounts of graft copolymers (A) cooling of PS/PA-6 blends, (B) heating of PS/PA-6 blends, (C) cooling of PS/PA-12 blends, and (D) heating of PS/PA-12 blends. (Values for *W/g* given are based on the total sample weights.)

Table IV Summarized DSC Results for PS/PA-6 Blends

Sample	T_g (PS) (°C)	T_{melt} (PA-6) (°C)	ΔH_f (PA-6) (J/g)[a]	T_c (PA-6) (°C)	ΔH_c (PA-6) (J/g)[a]	T_{melt} (PEO) (°C)	ΔH_f (PEO) (J/g)[a]
PS	102	—	—	—	—	—	—
PA-6	—	221	58	168	52	—	—
PS/PA-6 80/20	102	220	11	189	11	—	—
PS/PA-6/SEO18 80/20/1	100	218	12	185	8	—	—
PS/PA-6/SEO18 80/20/3	100	220	11	188	10	52	1.3
PS/PA-6/SEO18 80/20/5	100	220	10	C	C	54	2.3
PS/PA-6/SEO20 80/20/1	100	220	9	C	C	—	—
PS/PA-6/SEO20 80/20/3	99	217	10	C	C	T	T
PS/PA-6/SEO20 80/20/5	99	217	11	C	C	39	0.5
PS/PA-6/SEO21 80/20/1	102	220	9	187	11	—	—
PS/PA-6/SEO21 80/20/3	97	217	11	187	12	39	0.7
PS/PA-6/SEO21 80/20/5	98	217	10	186	11	34	1.1

C, cold crystallization, difficult to evaluate; T, traces, difficult to evaluate.
[a] Based on the total sample weight.

cence equilibrium.[15,19] The role of a compatibilizer is to lower the interfacial tension and to decelerate the coalescence process. Some domain aggregates were noticed among isolated PA domains from compatibilized compression molded PS/PA-6 blends (Fig. 10). In the corresponding uncompatibilized blends, no evidence for aggregation was found. The presence of the aggregates do not indicate a higher degree of coalescence, but rather implies that the domains are more stable in a compatibilized system. Thus, when two domains collide during mixing or processing, a stabilizing graft copolymer layer between the aggregated domains may inhibit coalescence.

PA Crystallization

Cooling and heating DSC thermograms of PS and PA-6 together with thermograms of uncompatibilized and compatibilized PA-6 blends are shown in Figure 11(A,B). The corresponding thermograms for PA-12 blends can be seen in Figure 11(C,D). The results from the evaluations of the thermograms are summarized in Tables IV and V for the PA-6 and PA-12 blends, respectively.

The glass transition of pure PS appears at 102°C. Pure PA-6 and PA-12 have melting endotherms at 221 and 176°C, respectively, and crystallization exotherms at 168 and 139°C, respectively. In the uncompatibilized blends, crystallization of the PA phase takes place at higher temperatures, as compared to the pure PAs, 189°C for PA-6 and 155°C for PA-12. It appears as the PS interface promotes the crystallization process, and allows it to start at higher temperatures. Although there was a difference in crystallization temperatures between the PAs in the pure state and in the uncompatibilized blends, no difference in the melting temperature was observed. The heat of fusion (ΔH_f) based on the PA contents of the blends are roughly the same as for the corresponding pure PAs.

Crystallization of the dispersed PA phase in blends containing graft copolymer SEO18 or SEO20 became increasingly difficult at increasing compatibilizer contents. As can be seen in Figure 11(A,C), this effect was most pronounced for PS/PA-6 blends containing SEO20. The PA-6 crystallization peak of the uncompatibilized PS/PA-6 blend at 189°C [Fig. 11(A)] was split into two peaks when 1 wt % of SEO20 was present, the original peak at 189°C and a new at 168°C. When 3 wt % of SEO20 was present, the crystallization temperatures of the two crystal fractions shifted toward lower temperatures, and a third crystallization peak emerged directly after the PS glass transition at 80°C. When the compatibilizer content was increased further up to 5 wt %, the two peaks at 189 and 168°C vanished almost completely while the peak at 80°C continued to increase. Retarded crystallizations at lower temperatures than normal of dispersed semicrystalline phases in immiscible blends have been observed previously.[23,24] The so-called cold crystallization behavior was not observed in blends containing graft copolymer SEO21, which was inactive as a compatibilizer, as previously noted. The cold crystallization neither influenced the degree of crystallinity nor the melting temperatures of the PA phases. No significant effect on the PS glass transition was noted.

Table V Summarized DSC Results for PS/PA-12 Blends

Sample	T_g (PS) (°C)	T_{melt} (PA-12) (°C)	ΔH_f (PA-12) (J/g)[a]	T_c (PA-12) (°C)	ΔH_c (PA-12) (J/g)[a]	T_{melt} (PEO) (°C)	ΔH_f (PEO) (J/g)[a]
PS	102	—	—	—	—	—	—
PA-12	—	176	53	139	53	—	—
PS/PA-12 80/20	100	176	10	155	11	—	—
PS/PA-12/SEO18 80/20/1	100	177	9	153	10	—	—
PS/PA-12/SEO18 80/20/3	99	176	8	153	9	51	0.8
PS/PA-12/SEO18 80/20/5	98	175	8	C	C	49	2.0
PS/PA-12/SEO20 80/20/1	101	177	10	154	11	—	—
PS/PA-12/SEO20 80/20/3	101	178	8	154	9	T	T
PS/PA-12/SEO20 80/20/5	99	176	8	152	9	37	0.4
PS/PA-12/SEO21 80/20/5	98	177	7	155	8	38	1.4
PS/PA-12 80/20 extruded	100	177	9	C	C	—	—
PS/PA-12/SEO20 80/20/3 extruded	100	177	7	C	C	—	—

C, cold crystallization, difficult to evaluate; T, traces, difficult to evaluate.
[a] Based on the total sample weight.

Crystallization of a dispersed semicrystalline phase in an immiscible blend generally depends on the type, number, and distribution of nucleating sites, as well as on the degree of dispersion.[14] As the dispersion becomes finer, for example as a result of the addition of a compatibilizer, the domains may outnumber the nucleating sites. Crystallization may then be controlled by another type of heterogeneity.[14] Both PA-6 and PA-12 crystallized at a higher temperatures in the uncompatibilized blends compared to the pure PAs. It is conceivable that at least some crystallization was nucleated at the PS/PA interface. In fact, spherulitic surface structures were observed on the surfaces of PA domains from uncompatibilized blends and blends containing graft copolymer SEO21 (Fig. 12). The spherulitic surface structures, which were most pronounced on PA-12 domains, were about 5–10 μm in diameter. This corresponds to a nucleating site density of about 1 site per 50 $(\mu m)^2$ at the interface. Although most of the surface of the domains was covered with spherulites, some smooth surface areas on the domains without spherulites were also observed (see Fig. 12). Crystallization of a single PA domain may therefore be nucleated at the interface as well as inside the domain. In the presence of graft copolymer at the in-

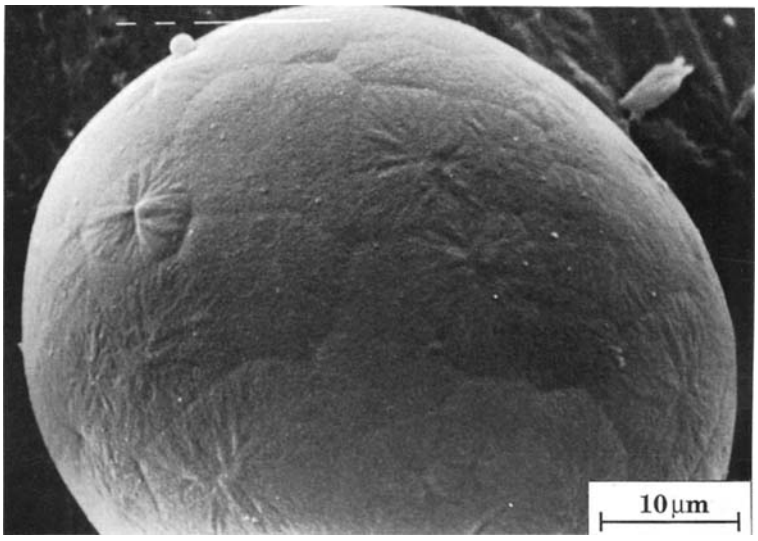

Figure 12 SEM micrograph of a free PA-12 domain, isolated from the compression molded PS/PA-12 blend with 5 wt % SEO21, showing a spherulitic surface structure.

Table VI Effect of Mixing Method on PA-12 Domain Sizes

Diameter	Extruded with 0% SEO20	Extruded with 3% SEO20	Brabender Mixed with 0% SEO20	Brabender Mixed with 3% SEO20
$\bar{R}_n$	1.0	0.8	1.3	0.8
$\bar{R}_w$	3.4	1.5	3.8	1.7

terface, the sharp boundary between PS and PA would become less distinct. The high-temperature crystallization disappeared gradually as the graft copolymer content was increased, and the spherulitic surface structures could no longer be observed. Instead, PA crystallization was observed at the PS glass transition [Fig. 11(A)]. The interfacial mobility should decrease significantly below the PS glass transition, which would give opportunity for PA crystallization. A similar low-temperature crystallization of a dispersed PA-6 phase in a compatibilized polypropylene/PA-6 blend has previously been reported.[24] In this system, PA was found to crystallize coincidently with polypropylene at the polypropylene crystallization temperature.

PEO Side Chain Crystallinity

At graft copolymer contents of 3 and 5 wt % in the blends, PEO crystallinity can be observed by DSC as melting endotherms at somewhat lower temperatures than for the pure graft copolymers (Table I). The melting endotherms indicate that the graft copolymers are phase separated. Preliminary results from a TEM investigation revealed phase structures, about 50–200 nm in size, present in the PS phase of a PS/PA-6 blend containing 5 wt % SEO18. The structures, which were absent in the uncompatibilized blend, were of similar appearance as the micellar aggregates found in binary blends containing graft copolymers.[25] For the PS/PA-6 blend containing 5 wt % SEO18, side chain crystallization of the graft copolymer was observed as a double peak between −10 and −30°C [Fig. 11(A)].

A compatibilizer may be localized as thin layers at interfaces in an immiscible blend, which has been confirmed by direct observation using TEM.[26] The graft copolymers SEO18 and SEO20 can be assumed to be partly located at the interfaces, as presumed in eq. (3). The location of graft copolymer SEO21 is more uncertain. As pointed out previously, the copolymer apparently is unable to stabilize the blends, and thus it is unlikely that it is located at the interfaces. Most probably it has formed a separate phase dispersed in the PA and/or PS phases.

Effect of Mixing Method

The size and shape of the domains in compatibilized immiscible blends are usually strongly dependent on the mixing method.[15] The PA domain sizes for PA-12 blends are reported in Table VI. The blends were prepared by Brabender mixing as well as by extrusion, before compression molding. The difference between the two preparation methods regarding the PA domain sizes was small for the compatibilized blends. For the uncompatibilized blends, Brabender mixing yields slightly larger domains in comparison with extrusion. It may be concluded that the mixing method seems to have little influence on the morphology after compression molding in the present case.

In contrast to the results obtained for the Brabender mixed blends, cold crystallization was observed for the extruded PS/PA-12 blends [Fig. 11(C)]. Because there were only marginal differences in the PA domain sizes after compression molding, these cannot account for the appearance of cold

Table VII Impact and Tensile Data

Sample	Unnotched Charpy Impact Strength (kJ/m^2)	Notched Charpy Impact Strength (kJ/m^2)	Stress at Break (MPa)	Elongation at Break (%)
PS/PA-12 (80/20)	4.2 ± 0.3	2.6 ± 0.3	31 ± 1	5.5 ± 0.3
PS/PA-12/SEO20 (80/20/3)	6.9 ± 0.3	3.3 ± 0.3	31 ± 1	5.4 ± 0.3
PS	4.7 ± 0.3	3.8 ± 0.3	48 ± 1	3.5 ± 0.2
PA-12	No break	No break	37 ± 2[a]	180 ± 7

Values are mean ± standard deviation.
[a] Yield point at 37 MPa.

crystallization. In our view the most probable cause for the difference in crystallization behavior may be that the extruded blends have less amounts of nucleating impurities, as compared to those prepared by Brabender mixing.

Mechanical Properties

Table VII contains data from impact and tensile testing of injection molded PS/PA-12 blends containing 0 and 3 wt % of SEO20. On the addition of graft copolymer, the Charpy impact strength of the blend increased by 64%, and the Charpy notched impact strength by 27%. The observed increase in impact strength was not parallelled by an expected increase in the elongation at break. We have found no reports on the mechanical properties of compatibilized PS/PA-12 blends. Chen and White[3] studied the mechanical properties of PS/PA-6 (80/20) blends compatibilized with different reactive and nonreactive polymers. They found that the elongation at break and the impact strength were actually lower for blends compatibilized with styrene–acrylonitrile and styrene–maleic anhydride copolymers, as compared with the uncompatibilized blend. Blends compatibilized with 5% of a maleic anhydride modified styrene–hydrogenated butadiene–styrene triblock copolymer showed a 205% increase in the elongation at break, but no significant increase in impact strength.

CONCLUSIONS

PEO interacts with PA-6 through hydrogen bonding, with PA-6 amide hydrogens acting as bond donors and PEO ether oxygens as bond acceptors. Similar interactions presumably also exist between PEO and PA-12, although the results are not as conclusive as with PA-6. The intermolecular hydrogen bonding induces a partial miscibility of PEO with PA that gives opportunities for using poly(styrene-*graft*-ethylene oxide) as a compatibilizer in PS/PA-6 and PS/PA-12 blends.

Additions of graft copolymers with proper structural features effectively reduce PA domain sizes. Also, the PA domain size distributions were more uniform in the compatibilized blends. A saturation effect was noted for both PA-6 and PA-12 blends at 3 wt %, after which no further reduction in domain sizes could be noted. The graft copolymers phase separate from the compatibilized blends at concentrations above the saturation concentration, forming micellar aggregates. This shows that the solubility of the graft copolymers in the blends is low when the PS/PA interfaces are saturated.

The crystallization of the PA phases was found to be influenced by the degree of compatibilization. The PS/PA interface in uncompatibilized blends seemed to have a nucleating effect on the PA crystallization, allowing it to take place at higher temperatures than for pure PA. When increasing amounts of graft copolymer was added to the blends, this effect gradually disappeared and the PA crystallization temperatures were lowered. The increased additions of graft copolymer to the blends should also lead to an increase in the interfacial coverage by the graft copolymer, and thereby a reduction in PA domain sizes. The PA crystallization may be suppressed by a gradual disappearance of the nucleating effect of the PS/PA interface and a reduction in the number of nucleating sites per PA domain in the blends.

We would like to thank Bjurhagens Fabrikers AB, especially Mr. Bengt Jonsson, for use of their Brabender mixer, and Dr. Bertil Ohlsson at our department for helping us with the extruder. The financial support by the Swedish National Board for Industrial and Technical Development, NUTEK, is gratefully acknowledged.

REFERENCES

1. D. R. Paul in *Polymer Blends,* Vol. 2, D. R. Paul and S. Newman, Eds., Academic Press, New York, 1978, Chap. 12.
2. L. A. Utracki, *Polymer Alloys and Blends,* Hansers Publ., Munich, 1989, Chap. 2.7.2.
3. C. C. Chen and J. L. White, *Polym. Eng. Sci.,* **33,** 923 (1993).
4. C. C. Chen, E. Fontan, K. Min, and J. L. White, *Polym. Eng. Sci.,* **28,** 69 (1988).
5. I. Park, J. W. Barlow, and D. R. Paul, *J. Polym. Sci., Polym. Phys. Ed.,* **30,** 1021 (1992).
6. F.-C. Chang and Y.-C. Hwu, *Polym. Eng. Sci.,* **31,** 1509 (1991).
7. F. Ide and A. Hasegawa, *J. Appl. Polym. Sci.,* **18,** 963 (1974).
8. R. Fayt and Ph. Teyssié, *J. Polym. Sci., Polym. Lett.,* **27,** 481 (1989).
9. M. M. Coleman, J. F. Graf, and P. C. Painter, *Specific Interactions and the Miscibility of Polymer Blends,* Technomic Publ. Company, Inc., Lancaster, PA, 1991.
10. J. Hu, P. C. Painter, M. M. Coleman, and T. D. Krizan, *J. Polym. Sci., Polym. Phys. Ed.,* **28,** 149 (1990).
11. G. Qipeng, F. Tianru, C. Tianlu, and F. Zhiliu, *Polym. Commun.,* **32,** 22 (1991).
12. P. Jannasch and B. Wesslén, *J. Polym. Sci., Polym. Chem. Ed.,* **31,** 1519 (1993).

13. M. M. Coleman, D. J. Skrovanek, and P. C. Painter, *Makromol. Chem., Macromol. Symp.*, **5,** 21 (1986).
14. H. Frensch, P. Harnischfeger, and B.-J. Jungnickel, in *Multiphase Polymers: Blends and Ionomers,* L. A. Utracki and R. A. Weiss, Eds., ACS, Washington DC, 1989, pp. 101–125.
15. A. P. Plochocki, S. S. Dagli, and R. D. Andrews, *Polym. Eng. Sci.*, **30,** 741 (1990).
16. L. C. Sawyer and D. T. Grubb, *Polymer Microscopy,* Chapman and Hall, London and New York, 1987, Chap. 4.
17. T. Tang and B. Huang, *Polymer,* **35,** 281 (1994).
18. J. M. Willis and B. D. Favis, *Polym. Eng. Sci.*, **28,** 1416 (1988).
19. G. I. Taylor, *Proc. Roy. Soc.*, **A146,** 501 (1934).
20. R. Fayt, R. Jérôme, and P. Teyssié, in *Multiphase Polymers: Blends and Ionomers,* L. A. Utracki and R. A. Weiss, Eds., ACS, Washington DC, 1989, Chap. 2.
21. S. C. Tang, C. P. Hu, and S. K. Ying, *Polym. J.*, **22,** 70 (1990).
22. D. G. Pfeiffer and M. Rabeony, *J. Appl. Polym. Sci.*, **51,** 1283 (1994).
23. M. Xantos, M. W. Young, and J. A. Biesenberger, *Polym. Eng. Sci.*, **30,** 355 (1990).
24. O. T. Ikkala, R. M. Holsti-Miettinen, and J. Seppälä, *J. Appl. Polym. Sci.*, **49,** 1165 (1993).
25. D. Braun, M. Fischer, and G. P. Hellmann, *Macromol. Symp.*, **83,** 77 (1994).
26. R. Fayt, R. Jerome, and Ph. Teyssié, *J. Polym. Sci., Polym. Lett. Ed.*, **24,** 25 (1987).

Received February 23, 1995
Accepted April 2, 1995